International Journal of Pharmaceutics 403 (2011) 66–72

Contents lists available at ScienceDirect

International Journal of Pharmaceutics

journal homepage: www.elsevier.com/locate/ijpharm

In line NIR quantification of film thickness on pharmaceutical pellets during a fluid bed coating process

Min-Jeong Lee[a], Da-Young Seo[a], Hea-Eun Lee[b], In-Chun Wang[b], Woo-Sik Kim[c], Myung-Yung Jeong[d], Guang J. Choi[a,b,*]

[a] Department of Smart Foods & Drugs, Inje University, Gimhae, Gyeongnam 621-749, South Korea
[b] Department of Pharmaceutical Engineering, Inje University, Gimhae, Gyeongnam 621-749, South Korea
[c] Department of Chemical Engineering, ILRI, Kyung Hee University, Yongin, Gyeonggi 446-701, South Korea
[d] WCU Department of Cogno Mechatronics Engineering, Pusan National University, Busan 609-735, South Korea

ARTICLE INFO

Article history:
Received 10 August 2010
Received in revised form
30 September 2010
Accepted 15 October 2010
Available online 28 October 2010

Keywords:
Fluid-bed coating
Coating thickness
PAT
NIR
Pellets
CLSM
PSA

ABSTRACT

Along with the risk-based approach, process analytical technology (PAT) has emerged as one of the key elements to fully implement QbD (quality-by-design). Near-infrared (NIR) spectroscopy has been extensively applied as an in-line/on-line analytical tool in biomedical and chemical industries. In this study, the film thickness on pharmaceutical pellets was examined for quantification using in-line NIR spectroscopy during a fluid-bed coating process. A precise monitoring of coating thickness and its prediction with a suitable control strategy is crucial to the quality assurance of solid dosage forms including dissolution characteristics.

Pellets of a test formulation were manufactured and coated in a fluid-bed by spraying a hydroxypropyl methylcellulose (HPMC) coating solution. NIR spectra were acquired via a fiber-optic probe during the coating process, followed by multivariate analysis utilizing partial least squares (PLS) calibration models. The actual coating thickness of pellets was measured by two separate methods, confocal laser scanning microscopy (CLSM) and laser diffraction particle size analysis (LD-PSA). Both characterization methods gave superb correlation results, and all determination coefficient (R^2) values exceeded 0.995. In addition, a prediction coating experiment for 70 min demonstrated that the end-point can be accurately designated via NIR in-line monitoring with appropriate calibration models. In conclusion, our approach combining in-line NIR monitoring with CLSM and LD-PSA can be applied as an effective PAT tool for fluid-bed pellet coating processes.

1. Introduction

Film coating processes are used for various purposes, such as detecting appearance changes, masking taste, and improving stability or drug delivery behavior in the pharmaceutical industry. The performance of end products put through a coating process is greatly dependent upon the film coating thickness, its uniformity and morphology. For instance, coatings that are too thin would not meet the anticipated protection for sustained release, whereas coatings that are too thick could result in delayed disintegration or dissolution, as well as poor efficiency in terms of coating time and materials consumed (Andersson et al., 1999).

Accordingly, coating thickness must be precisely controlled to ensure the quality of solid dosage form products. In-line monitoring is important, not only for the products quality but also for a better understanding of the coating process. An improvement in process understanding was one of the key goals of FDA's PAT initiative in 2004 (FDA, 2004). In many cases, pharmaceutical processes were understood better via process monitoring (Maurer and Leuenberger, 2009).

The monitoring of tablet coating processes has been extensively investigated. Various analytical tools have been employed to examine coating characteristics on tablets, including attenuated total reflection-infrared (ATR-IR) imaging (Reich, 2002), laser induced breakdown spectroscopy (LIBS) (Mowery et al., 2002), confocal laser scanning microscopy (CLSM) (Ruotsalainen et al., 2003), Raman spectroscopy (Romero-Torres et al., 2005; El-Hagrasy et al., 2006; Kauffman et al., 2007), near-infrared (NIR) spectroscopy (Kirsch and Drennen, 1995, 1996; Perez-Ramos et al., 2005; Roggo et al., 2005; Cogdill et al., 2007; Lee et al., 2010), and terahertz pulsed imaging (TPI) (Fitzgerald et al., 2005; Zeitler et al., 2006; Cogdill et al., 2007; Ho et al., 2007, 2008, 2009b).

On the other hand, there have been only few studies that analyze or monitor the coating of granules or pellets. Image analysis meth-

* Corresponding author at: Department of Pharmaceutical Engineering, Inje University, B-409, 607 Obang-dong, Gimhae, Gyeongnam 621-749, South Korea.
Tel.: +82 11 9912 6429; fax: +82 55 327 4955.
E-mail address: pegchoi@inje.ac.kr (G.J. Choi).

0378-5173/$ – see front matter © 2010 Elsevier B.V. All rights reserved.
doi:10.1016/j.ijpharm.2010.10.022

ods were primarily used to determine the coating thickness of the pellets. Andersson et al. (2000b) utilized fluorescence microscopy for the analysis of variations in coating thickness on a single pellet and between different pellets. Hierarchical analysis of variance was used to obtain diverse information on the coating quality. In addition, variations in release rate associated with the geometrical variations in pellets were correlated with the image date to predict the release rate using a mathematical model (Andersson et al., 2000b).

Recently, a study employing the confocal laser scanning microscopy (CLSM) and terahertz pulsed imaging (TPI) to analyze pellet coatings was reported (Laksmana et al., 2009). CLSM was applied to quantify the coating thickness and distribution, and was determined to be a fast and effective analysis tool. The coating functionality was predicted as well. Another study demonstrated that the CLSM data can be used to characterize the coating quality as well as the coating thickness to 1–1.5 μm (Depypere et al., 2009). TPI was used to investigate nondestructively the effects of the coating thickness, its uniformity, and the curing on in vitro drug release behavior for sustained-release pellets (Ho et al., 2009a). Ho et al. (2009a) demonstrated that appreciable variations in film coating thickness, surface roughness, and homogeneity can be detected by TPI measurements.

The majority of pellet coating studies were focused on presenting methods for coating thickness analysis or on correlating release behavior with the coating thickness. Alternatively, Andersson et al. (2000a) carried out experiments to monitor a fluid-bed pellet coating process based on their previous study. Pharmaceutical pellets were measured by NIR spectroscopy with a diffuse reflectance fiber-optic probe mounted in a fluidized bed process vessel. Process conditions were systematically varied according to an experimental design scheme. Their multivariate batch calibration model by partial least squares (PLS) yielded good predictability of the coating thickness with a best model fit (R^2 = 0.97) (Andersson et al., 2000a).

The feasibility of an acoustic monitoring for a production-scale fluidized bed coating process was investigated (Naelapää et al., 2007). Potassium chloride (KCl) crystals were coated with ethylcellulose (EC). Sensor signals were correlated with the estimated amount of coating film and the release percentage. The best PLS regression with the estimated amount of coating thickness using a high frequency accelerometer resulted in a correlation coefficient as high as 0.95 and a root mean square error of prediction (RMSEP) of 0.6–6%.

As mentioned above, there has not been a superb correlation and calibration model for a fluid-bed pellet coating process. An end point prediction would be considered practically feasible when the correlation coefficient exceeds 0.99 with a small error value. One of the primary causes for poor correlation might be due to differences in statistically handling NIR spectra acquired from the dynamic fluid-bed process. Averaging with or without clustering seems to be the optimal method for correlating and predicting the coating thickness on tablets based on NIR spectra (Lee et al., 2010).

In this study, we correlate in-line NIR spectra from a fluid-bed pellet coating process with two separate methods for determining coating thickness; laser diffraction particle size analysis (LD-PSA) and CLSM image analysis. Averaging with clustering was applied with PLS calibration to improve the correlation level. The predictability of our calibration models was tested as well.

2. Materials and methods

2.1. Materials

Granule-shaped pellets to be coated were manufactured combining three pharmaceutical ingredients: microcrystalline cellulose (MCC; HEWETEN® 101; JRS Pharma, Rosenberg, Germany), lactose monohydrate (DMV-Fonterra, Netherlands) and polyvinylpyrrolidone (PVP; Kollidon® K-30; BASF Corp., Ludwigshafen, Germany). Two polymers were selected as coating materials: polyethylene glycol (PEG 4000; Shinyo, Japan) and hydroxypropyl methylcellulose (HPMC; Pharmacoat® 606; Shin-Etsu, Japan). Fluorescein sodium salt (Uranin; Fluka Chemie AG, Buchs, Switzerland) was added in trace amounts to enhance the images for CLSM analysis.

Table 1
Composition of pellets to be coated.

Ingredient	Weight %
Lactose monohydrate	70
Microcrystalline cellulose (MCC)	25
Polyvinylpyrrolidone (PVP)	5
Distilled water	50 (of powder mixture)

2.2. Pellet preparation

First, for size control, MCC, lactose and PVP were passed through a US standard 30-mesh sieve prior to a V-blender (MD-Korea, Korea) powder blending for 20 min. Subsequently distilled water was added intermittently while wet blending was performed manually in a shaker for 10 min. The composition of the powder mixture with the amount of water added for the wet granulation is summarized in Table 1.

The wet blended mass was sieved through a custom-built oscillator (MD-Korea, Korea) equipped with a 0.8 mm screen, followed by drying the wet granules at 60 °C for 12 h. The dried granules were passed through the oscillator equipped with a 1 mm screen once more. Finally, pellet sieving was carried out employing an automatic sieve shaker (Sam Jin Sci., Korea) with two screens in order to collect exclusively those pellets with sizes between 600 μm and 710 μm.

2.3. Pellet coating

The HPMC-based coating solution was prepared by slowly adding HPMC into a 1% (w/w) PEG solution with mild agitation to make a 10% HPMC solution. When the HPMC was fully dissolved in solution, a trace amount (1.5 mg in 300 mL solution) of fluorescein sodium salt was added.

Pellet coating was performed in a custom-made fluid bed coater (MD-Korea, Korea) of the bottom spray type. Fig. 1 is a schematic diagram of our fluid-bed pellet coating process with in-line NIR monitoring. Pellets of 250 g were used for each coating operation with the experimental conditions given below:

- inlet air temperature = 50 °C
- air flow rate = 60 m^3/h
- spray rate of coating solution = 1 mL/min
- atomization pressure = 5 psi.

After stabilizing the fluidized motion as well as the inside temperature at 50 °C by a 5 min preconditioning step, each coating process was operated for 90 min in total with periodic samplings of 4 g every 15 min. Every coating experiment was repeated under exactly the same conditions to test reproducibility. In addition, a separate coating operation was carried out for 70 min without sampling solely to validate our calibration model as well as its prediction capability.

2.4. NIR spectra collection

A FT-NIR spectrometer (FTPA 2000-260; ABB Bomem, Quebec, Canada) equipped with a tungsten–halogen source and an InGaAs

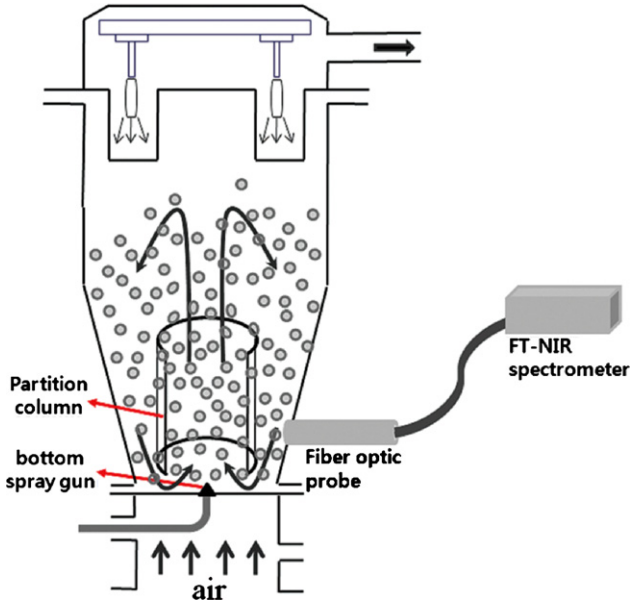

Fig. 1. Schematic diagram of the fluid-bed coating process with NIR spectrometer.

detector was used for in-line monitoring. NIR spectra were collected in real-time during the coating process via a fiber-optic diffuse reflectance probe (FOCON FO; ABB Bomem) that was connected to the fluid-bed coater as shown in Fig. 1.

All NIR in-line spectra were continuously collected and handled with GRAMS/AI 7.00 software (Galactic Ind., Salem, NH, USA). Each spectrum was acquired by averaging 32 scans with a resolution of 64 cm^{-1}, over the range of 4000–14,000 cm^{-1}. Spectral preprocessing and analyzing work to establish calibration models was performed using PLSplus/IQ program provided with the GRAMS/AI 7.00 software.

2.5. Confocal laser scanning microscopy (CLSM) image analysis

The Zeiss LSM 510-META (Carl Zeiss, Jena, Germany) was used for CLSM image analysis. The system was operated with an argon laser of 30 mW as the maximum power. In addition, the scan configurations were as follows:

- laser output = 50%
- transmission = 10%
- beam splitter HFT 405/488
- emission filter LP 505.

All confocal fluorescence images were taken with a EC Plan-Neofluar 10x/0.30 M27 objective lens and were acquired as 512 × 512 pixels through the software LSM 510 version 3.2 (Carl Zeiss, Germany). Recorded images were analyzed with the software ImageJ 1.43u (National Institutes of Health, USA). Image processing and calculations of coating thickness were performed by the protocol described by Depypere et al. (2009). In brief, the raw image was converted to a binary image, and subsequently the auto threshold was applied. Then each image was provided with two gray values that are black core background (0) and white coating (255). In the resulting binary image, an oval was constructed along the outside boundary of the coated pellet. The oval and its centroid were linked by a number of straight lines. The pixel gray values corresponding to the coating layer were determined along these radii, and the resulting thicknesses along these radii in pixels were converted to measurements in micrometers to afford the coating thickness distribution of a single pellet.

As recommended by Lamprecht et al. (2000), 15 pellets from each sample were selected to undergo CLSM image analysis. For every single pellet, 360 values of coating thickness were calculated.

2.6. Pellet size measurement

Another estimation of coating thickness was conducted by pellet size measurements. The average coating thickness was calculated from the difference in pellet size before and after coating. The particle size and distribution in a dry state was determined with a Laser Diffraction Particle Size Analyzer (LD-PSA; LS13 320; Beckman Coulter Inc., Miami, FL, USA).

3. Results and discussion

3.1. Pellet size and coating thickness via LD-PSA

As described earlier, 4 g of pellets were sampled every 15 min during the bottom-spray coating operation. A major portion of sampled pellets was reserved for various characterization studies such as particle size analysis. Table 2 summarizes the results of pellet size analysis. Each average value was calculated from triplicate measurements including the uncoated pellets. Average pellet diameters at 10%, 50%, and 90% cumulative volumes are referred to as D10, D50, and D90, respectively. In addition, the term 'span' was defined as (D90 – D10)/D50 to describe the width of size distribution. A span value less than one implies a narrow size distribution.

Interestingly, although we selected dried pellets of 600–710 μm for coating via sieve screening, the LD-PSA results signified that the diameter of uncoated pellets ranged between 500 and 800 μm. This discrepancy occurs primarily because the LD-PSA calculates the pellet size assuming a perfectly spherical shape, of which many pellets were not. In fact, a typical aspect ratio of uncoated pellets was estimated as low as 0.5.

Because each LD-PSA result showed a normal distribution shape, the D50 value was used as the average pellet diameter at each sampling time. The average coating thickness was calculated as half the difference between D50 values of uncoated and coated pellets. Overall, the average particle size, and hence the average coating thickness, increased proportionally to the coating time.

As seen in Table 2, D10 values did not increase constantly, but rather moved up and down, presumably because smaller fragments might have been formed by collisions between pellets during their fluidized motions. On the other hand, the span value was maintained at less than 0.6 until the later stage of the coating operation.

Table 2
Coating thickness via LD-PSA.

	0 min	15 min	30 min	45 min	60 min	75 min	90 min
D10 (μm)	545.1	545.2	465.5	516.5	564.7	530.3	506.9
D50 (μm)	622.9	639.0	674.8	722.9	748.7	769.7	797.3
D90 (μm)	742.5	826.1	845.0	855.3	989.0	1153.1	1208.6
Span	0.3	0.4	0.6	0.5	0.6	0.8	0.9
Coating thickness (μm)	0	8.1	25.9	50.0	62.9	73.4	87.2

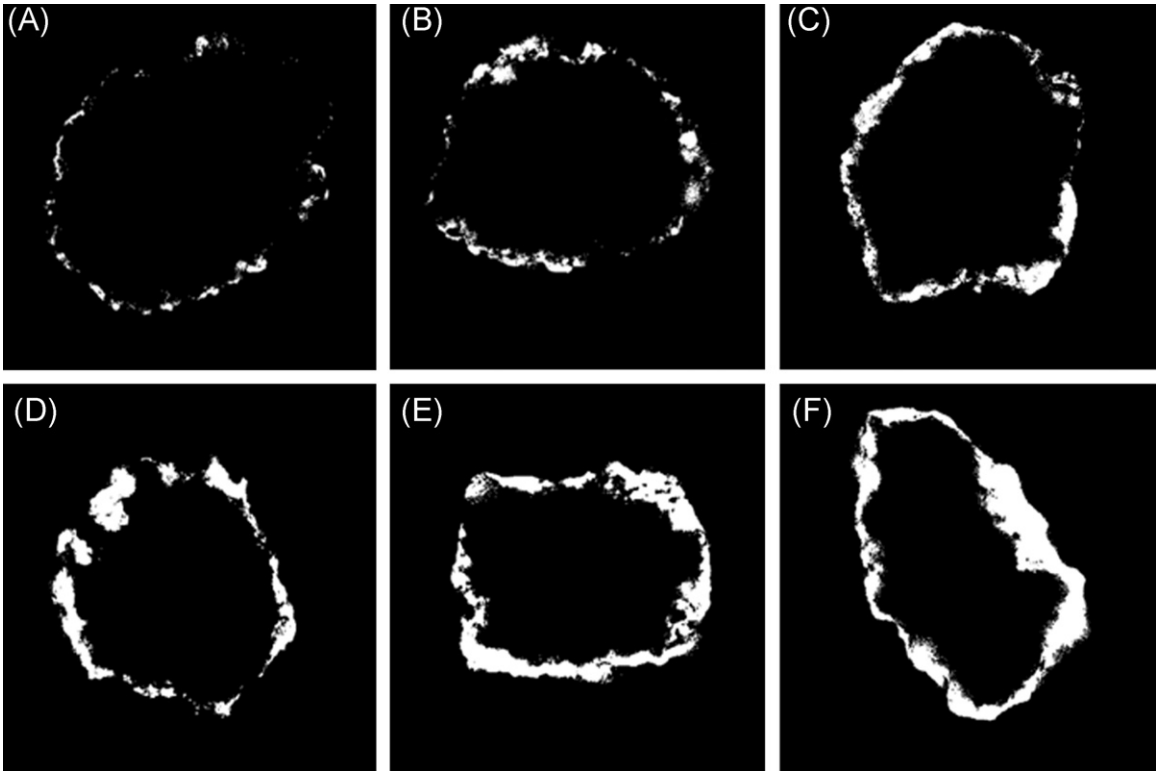

Fig. 2. CLSM images according to elapsed coating time. (A) 15 min, (B) 30 min, (C) 45 min, (D) 60 min, (E) 75 min, (F) 90 min.

3.2. CLSM image analysis

Pellets for the CLSM study were selected randomly from the sample collected at every 15 min. The uranin (fluorescein) in the coating solution was very effective as a fluorescent aid, enabling us to quantify the coating thickness from the CLSM image analysis. Fig. 2 illustrates typical CLSM images of pellets sampled at six time intervals. Each image consists of three regions: a white region for the coating layer, an inside black region for the pellet core, and an outside black region for the background. As expected, the coating layer gets thicker as the coating time becomes longer.

Because the shapes of the pellets were significantly irregular with a rough surface morphology, the white region did not grow uniformly in the radial direction. A certain extent of non-uniform coating of a single pellet is thus inevitable. Nevertheless, the digital image analysis showed an excellent correlation with the average coating thickness previously measured.

Table 3 summarizes the results of coating thickness measurements by CLMS image analysis. The upper part of the table is the result of a single pellet as shown in Fig. 2 whereas the lower part is for sampled 15 pellets. As mentioned earlier, the thickness measurement of each coated pellet was performed at 360 different angles. Then 360 thickness values are statistically treated to give a median or a mean thickness. As seen in the table, these two values are very different in some cases. The mean value was used as the average for our study. In addition, 5% of extreme values at both ends were excluded to give a 10% trimmed mean.

The average thickness values from 15 pellets at each sampling time are provided with standard deviation (SD) values. As expected, the average coating thickness increased as the coating time was extended. When the coating thickness was small, the standard deviation is high. Conversely, the SD value was small for the largest average thickness values.

As seen in Table 3, the inter-pellet variation of coating thickness is smaller than the intra-pellet variation. A similar result was observed in a study evaluating coating thickness by CLSM image analysis. It was mentioned that characterizing the intra-particle distribution is more important because it would help define the potential function of the coating (Laksmana et al., 2009). Accordingly, a small inter-particle variation in coating thickness seems to be desirable.

The average coating thickness values determined from the two methods are plotted with respect to the coating time as shown in Fig. 3. Although the two thickness values are close at short and

Table 3
Coating thickness via CLSM image analysis.

	15 min	30 min	45 min	60 min	75 min	90 min
$N = 1$ (Fig. 2)						
D10 (μm)	0	0	3.0	6.6	17.1	25.7
D90 (μm)	23.6	55.4	76.1	104.9	119.4	176.3
Median (μm)	4.0	11.8	33.6	37.6	67.1	76.1
Mean (μm)	9.2	21.2	35.9	49.8	69.7	93.6
10% Trimmed mean (μm)	7.0	15.9	33.2	43.4	67.4	86.8
$N = 15$						
Avg. of trimmed mean (μm)	5.7	16.9	32.2	46.0	68.7	84.9
SD (μm)	3.2	3.8	4.3	6.1	5.2	7.1

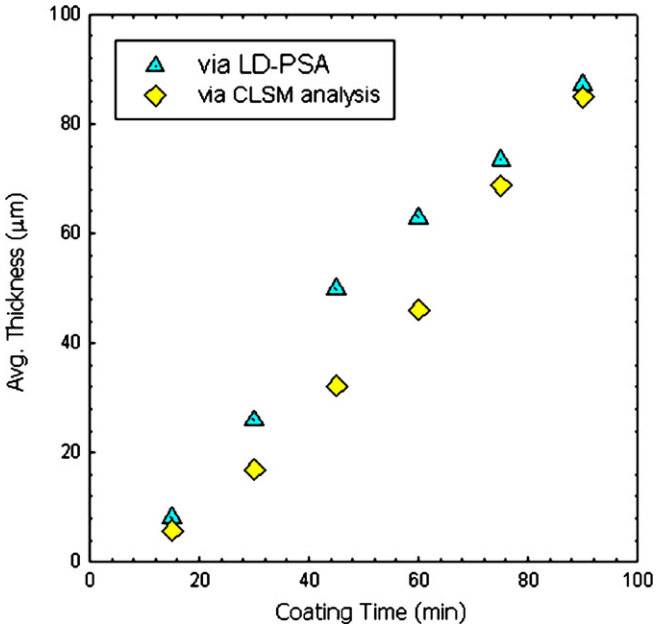

Fig. 3. Plots of avg. coating thickness versus coating time for LD-PSA and CLSM methods.

long coating times, there is a significant difference between thickness values for middle coating times. Considering that these two methods were performed using identical pellet samples, the discrepancy of around 30% at 45 min was particularly surprising. This discrepancy is quite reproducible, indicating that there is a wide disparity in the principles of these two methods for estimating coating thickness.

One thing to be noted is the poor uniformity of the coating at short coating times. A similar behavior was observed in a study on the monitoring of a film coating process (Seitavuopio et al., 2006). The surface roughness was reported to increase gradually for the initial 15–30 min until the whole solid surface was covered with a continuous film. Once the pellets were covered continuously, the coating proceeded smoothly in proportion to the time.

3.3. NIR spectra analysis

Over 1400 NIR spectra were collected during a typical coating process. For the analysis, 45 spectra corresponding to each sampling time were used i.e., one spectrum at the exact sampling time and 22 spectra of neighbors in both directions. It was reported that the performance of NIR monitoring for dynamic processes can be greatly improved by the averaging and clustering scheme (Lee et al., 2010). The NIR in-line spectra acquisition was not interrupted during the intermittent sampling operations because the NIR's detection area was away from the sampling location.

Fig. 4 illustrates the NIR spectra of coated pellets with the coating material. All spectra were pretreated with the baseline correction method. The lower part, consisting of 315 absorbance spectra (45 at each sampling time), shows that the spectra move upward as the coating proceeds. The spectral variation is most distinctive in the region of 6000–5000 cm^{-1}. All spectra were overlapped well to make seven distinct spectra groups. This confirms that the reproducibility of the NIR in-line spectra is good. In general, small and dense pellets such as ours are likely to give an excellent reproducibility in NIR monitoring of dynamic processes.

Fig. 5 shows the PC score plot as the result of principal component analysis (PCA) for the coating process. 315 spectra were preprocessed by baseline correction prior to PCA in the spectral range of 7500–5000 cm^{-1}. All score points are colored to distinguish each group. In brief, the whole coating process is represented by the change of a single clear component, that is, the coating thickness. As the coating proceeded, score points shifted from the upper left region to the lower right region. The PC1 took 96.68% while the PC2 contributed by 3.28% to the spectral variation. Accordingly, we anticipate an excellent correlation between the NIR in-line spectra and the coating thickness. Notably, there are no outliers in this PC score plot.

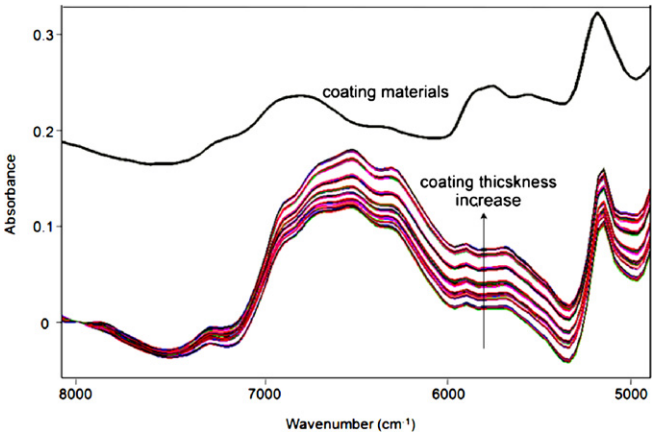

Fig. 4. Comparison of NIR spectra of the coating materials and pellets being coated.

3.4. Calibration model

Fig. 6 shows the correlation plots between thickness values from NIR monitoring and from two separate measurements. The 'actual coating thickness' in the horizontal axis denotes the measured thickness whereas the 'predicted coating thickness' in the vertical axis represents the thickness from NIR spectra. Baseline correction was applied as part of the preprocessing technique, and spectral regions of 7500–5000 cm^{-1} were selected to create calibration models with the partial least squares (PLS) regression. Cross validation was performed to determine the optimum number of factors. In our previous study, the clustering scheme with averaging was applied to improve the quality of calibration models. In this study, however, this clustering approach was not as effective because there were no obvious outlying data points.

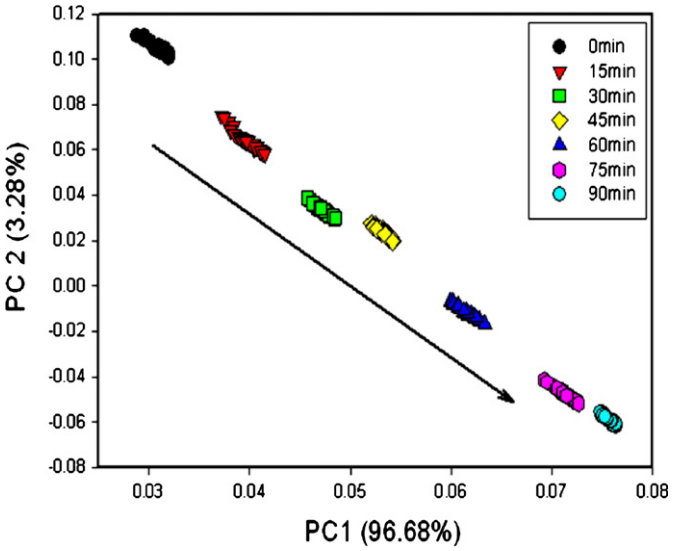

Fig. 5. Principal component score plot for the entire coating process.

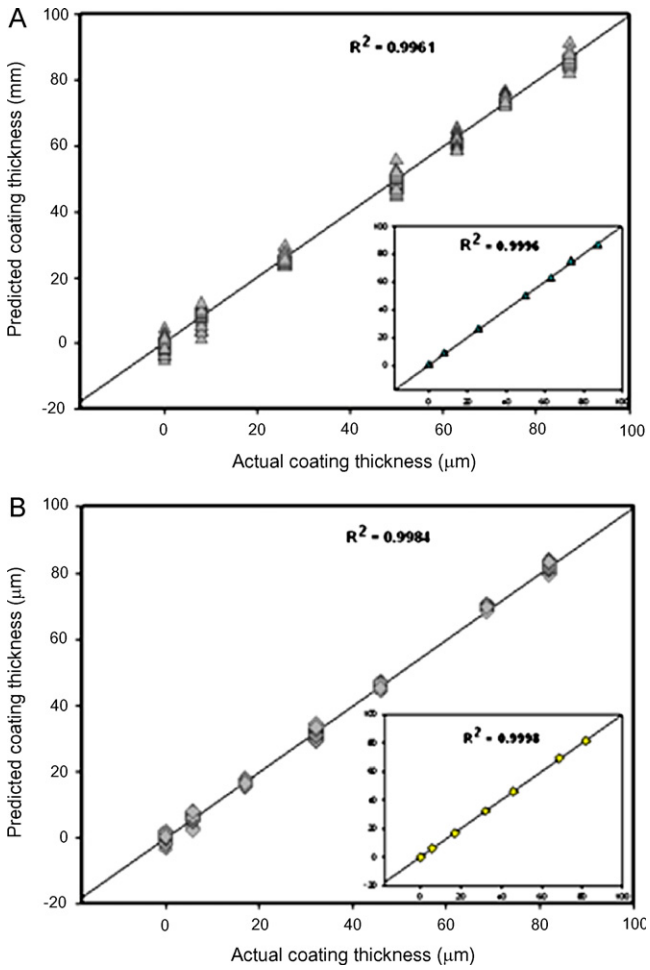

Fig. 6. Correlation plots of spectral coating thickness versus measured coating thickness from (A) LD-PSA and (B) CLSM methods.

As seen in Fig. 6, both LD-PSA (A) and CLSM (B) methods gave excellent calibration models with determination coefficient values (R^2) of 0.9961 and 0.9984, respectively. When 45 spectral points were averaged to make one point for each sampling time, the correlation gets better to greater than 0.9995 in both cases as shown in the boxed figures. Thus, the NIR in-line monitoring is a good predictor of coating thickness with an excellent correlation.

As mentioned earlier, there was a significant discrepancy in the thickness values between the two measurement methods in Fig. 3; namely, LD-PSA resulted in larger thickness values than CLSM. With the same NIR in-line spectra, however, two separate measurements gave calibrations with excellent correlation at the same time. This result suggests that the quality of the correlation (represented by R^2) is not strongly associated with the absolute values of a targeted attribute, but with its consistently changing pattern. This implies that the PLS-based multivariate analysis tool is excellent in terms of correlation whenever there is a consistently reproducible change in a quality attribute such as coating thickness.

With 45 spectra taken into account, an excellent correlation was achieved in both cases. We examined the effect of the spectra number on the correlation quality. In short, the correlation turned out reasonably acceptable ($R^2 > 0.994$) when the spectra number was greater than three (actual plots or tables are not given). Again, this result confirms that our fluid-bed pellet coating process is very reproducible with extremely few outlier points.

Table 4
Comparison of measured and predicted coating thickness values.

Classification	LD-PSA (μm)	CLSM (μm)
Measured coating thickness (No. of pellets = 50)	66.8 ± 5.1	60.5 ± 6.9
Predicted coating thickness		
(No. of spectra = 1)	72.8	57.4
(No. of spectra = 3)	65.5 ± 8.4	59.5 ± 6.0
(No. of spectra = 5)	65.6 ± 9.4	59.6 ± 5.2
(No. of spectra = 20)	66.8 ± 6.1	60.2 ± 6.0
(No. of spectra = 45)	68.3 ± 6.2	61.1 ± 6.7
Graphically calculated coating thickness at 70 min	70.5	61.0

3.5. Prediction of coating thickness

The predictability of our NIR-based calibration models was tested by a separate coating process with all experimental conditions the same except the coating time, which was set for 70 min. The fluid-bed process was continued for five more minutes for NIR spectra acquisition after the 70 min spraying was finished. Two prediction thickness values were obtained from two calibration models: the CLSM-based model and the PSA-based model. As shown in Table 4, five values are listed for each calibration model depending upon the number (from 1 to 45) of spectra taken into account.

Afterward, pellets of 30 g were examined in multiple orientations for actual coating thickness measurements. Among them, 50 pellets were used for the CLSM image analysis and the remainder subjected to the LD-PSA. Those thickness values are compared in Table 4. Compared to measured values, both predictions are excellent with a reasonable standard deviation when 20 spectra were averaged. For both models, predicted thickness values tend to increase slightly as the number of spectra averaged increases. A primary cause for this trend is yet to be found.

Other graphically predicted thickness values are compared in Table 4. These two values were calculated from Fig. 3 employing a graphical interpolation technique for each profile. Compared to measured thickness values, these are in excellent agreement.

4. Conclusion

Two characterization methods, LD-PSA and CLSM, were examined to establish calibration models to monitor precisely the coating thickness during a fluid-bed pellet coating process. According to our experimental results, LD-PSA tended to give a substantially larger thickness value than CLSM for the same pellets especially when the thickness ranged from 30 to 60 μm. Nevertheless, both calibration models gave excellent correlations with R^2 values exceeding 0.995. Therefore, it is clear that a reasonably consistent variation pattern should be a sufficient condition for a good calibration model. The averaging scheme was reasonably helpful as well.

The ability of our calibration models to predict thickness values was extremely good. When an appropriate number of spectra was taken for averaging (in our case, 20), accuracy was greater than 99%. Hence, it can be concluded that the fluid-bed pellet coating process can be precisely monitored via NIR in-line measurement aiming at an accurate prediction of the coating thickness as a high quality end point designation.

Acknowledgements

This research has been supported by Basic Science Research Program through the National Research Foundation of Korea (NRF) funded by the Ministry of Education, Science and Technology

(20090088240). In addition, we would like to acknowledge the instrumental assistance from ABB-Canada and ABB-Korea for in-line NIR spectroscopy.

References

Andersson, M., Folestad, F., Gottfries, J., Johansson, M.O., Josefson, M., Wahlund, K.G., 2000a. Quantitative analysis of film coating in a fluidized bed process by in-line NIR spectrometry and multivariate batch calibration. Anal. Chem. 72, 2099–2108.

Andersson, M., Holmquist, B., Lindquist, J., Nilsson, O., Wahlund, K.G., 2000b. Analysis of film coating thickness and surface area of pharmaceutical pellets using fluorescence microscopy and image analysis. J. Pharm. Biomed. 22, 325–339.

Andersson, M., Josefson, M., Langkilde, F.W., Wahlund, K.G., 1999. Monitoring of a thin film coating process for tablets using near infrared reflectance spectrometry. J. Pharm. Biomed. Anal. 20, 27–37.

Cogdill, R.P., Forcht, R.N., Shen, Y., Taday, P.F., Creekmore, J.R., Anderson, C.A., Drennen, J.K., 2007. Comparison of terahertz pulse imaging and near-infrared spectroscopy for rapid, non-destructive analysis of tablet coating thickness and uniformity. J. Pharm. Innov. 2, 29–36.

Depypere, F., Van Oostveldt, P., Pieters, J.G., Dewettinck, K., 2009. Quantification of microparticle coating quality by confocal laser scanning microscopy (CLSM). Eur. J. Pharm. Biopharm. 73, 179–186.

El-Hagrasy, A.S., Chang, S.-Y., Desai, D., Kiang, S., 2006. Raman spectroscopy for the determination of coating uniformity of tablets: assessment of product quality and coating pan mixing efficiency during scale-up. J. Pharm. Innov. 1, 37–42.

FDA, 2004. Guidance for Industry: PAT—A Framework for Innovative Pharmaceutical Development, Manufacturing, and Quality Assurance.

Fitzgerald, A.J., Cole, B.E., Taday, P.F., 2005. Nondestructive analysis of tablet coating thicknesses using terahertz pulsed imaging. J. Pharm. Sci. 94, 177–183.

Ho, L., Cuppok, Y., Muschert, S., Gordon, K.C., Pepper, M., Shen, Y., Siepmann, F., Siepmann, J., Taday, P.F., Rades, T., 2009a. Effects of film coating thickness and drug layer uniformity on in vitro drug release from sustained-release coated pellets: a case study using terahertz pulsed imaging. Int. J. Pharm. 382, 152–159.

Ho, L., Muller, R., Gordon, K.C., Kleinebudde, P., Pepper, M., Rades, T., Shen, Y.-C., Taday, P.F., Zeitler, J.A., 2008. Applications of terahertz pulsed imaging to sustained-release tablet film coating quality assessment and dissolution performance. J. Control. Release 127, 79–87.

Ho, L., Muller, R., Gordon, K.C., Kleinebudde, P., Pepper, M., Rades, T., Shen, Y.-C., Taday, P.F., Zeitler, J.A., 2009b. Terahertz pulsed imaging as an analytical tool for sustained-release tablet film coating. Eur. J. Pharm. Biopharm. 71, 117–123.

Ho, L., Muller, R., Romer, M., Gordon, K.C., Heinamaki, J., Kleinebudde, P., Pepper, M., Rades, T., Shen, Y.C., Strachan, C.J., Taday, P.F., Zeitler, J.A., 2007. Analysis of sustained-release tablet film coats using terahertz pulsed imaging. J. Control. Release 119, 253–261.

Kauffman, J.F., Dellibovi, M., Cunningham, C.R., 2007. Raman spectroscopy of coated pharmaceutical tablets and physical models for multivariate calibration to tablet coating thickness. J. Pharm. Biomed. Anal. 43, 39–48.

Kirsch, J.D., Drennen, J.K., 1995. Determination of film-coated tablet parameters by near-infrared spectroscopy. J. Pharm. Biomed. Anal. 13, 1273–1281.

Kirsch, J.D., Drennen, J.K., 1996. Near-infrared spectroscopic monitoring of the film coating process. Pharm. Res. 13, 234–237.

Laksmana, F.L., Van Vliet, L.J., Hartman Kok, P.J.A., Vromans, H., Frijlink, H.W., Voort Maarschalk, K., 2009. Quantitative image analysis for evaluating the coating thickness and pore distribution in coated small particles. Pharm. Res. 26, 965–976.

Lamprecht, A., Schafer, U., Lehr, C.M., 2000. Characterization of microcapsules by confocal laser scanning microscopy: structure, capsule wall composition and encapsulation rate. Eur. J. Pharm. Biopharm. 49, 1–9.

Lee, M.-J., Park, C.-R., Kim, A.-Y., Kwon, B.-S., Bang, K.-H., Cho, Y.-S., Jeong, M.-Y., Choi, G.J., 2010. Dynamic calibration for the in-line NIR monitoring of film thickness of pharmaceutical tablets processed in a fluid-bed coater. J. Pharm. Sci. 99, 325–335.

Maurer, L., Leuenberger, H., 2009. Terahertz pulsed imaging and near infrared imaging to monitor the coating process of pharmaceutical tablets. Int. J. Pharm. 370, 8–16.

Mowery, M.D., Sing, R., Kirsch, J., Razaghi, A., Bechard, S., Reed, R.A., 2002. Rapid at-line analysis of coating thickness and uniformity on tablets using laser induced breakdown spectroscopy. J. Pharm. Biomed. Anal. 28, 935–943.

Naelapää, K., Veski, P., Pedersen, J.G., Anov, D., Jørgensen, P., Kristensen, H.G., Bertelsen, P., 2007. Acoustic monitoring of a fluidized bed coating process. Int. J. Pharm. 332, 90–97.

Perez-Ramos, J.D., Findlay, W.P., Peck, G., Morris, K.R., 2005. Quantitative analysis of film coating in a pan coater based on in-line sensor measurements. AAPS PharmSciTech 6, E127–E136.

Reich, G., 2002. Potential of attenuated total reflection infrared and near-infrared spectroscopic imaging for quality assurance/quality control of solid pharmaceutical dosage forms. Pharm. Ind. 64, 870–874.

Roggo, Y., Jent, N., Edmond, A., Chalus, P., Ulmschneider, M., 2005. Characterizing process effects on pharmaceutical solid forms using near-infrared spectroscopy and infrared imaging. Eur. J. Pharm. Biopharm. 61, 100–110.

Romero-Torres, S., Perez-Ramos, J.D., Morris, K.R., Grant, E.R., 2005. Raman spectroscopic measurement of tablet-to-tablet coating variability. J. Pharm. Biomed. Anal. 38, 270–274.

Ruotsalainen, M., Heinamaki, J., Guo, H., Laitinen, N., Yliruusi, J., 2003. A novel technique for imaging film coating defects in the film–core interface and surface of coated tablets. Eur. J. Pharm. Biopharm. 56, 381–388.

Seitavuopio, P., Heinamaki, J., Rantanen, J., Yliruusi, J., 2006. Monitoring tablet surface roughness during the film coating process. AAPS PharmSciTech 7, E1–E6.

Zeitler, J.A., Shen, Y., Baker, C., Taday, P.F., Pepper, M., Rades, T., 2006. Analysis of coating structures and interfaces in solid oral dosage forms by three dimensional terahertz pulsed imaging. J. Pharm. Sci. 96, 330–340.